Sensors and Actuators A 265 (2017) 211–216

Contents lists available at ScienceDirect

Sensors and Actuators A: Physical

journal homepage: www.elsevier.com/locate/sna

Static and dynamic calibration of a MEMS calorimetric shear-stress sensor

Julien Weiss[a,*], Emmanuel Jondeau[b], Alain Giani[c], Benoît Charlot[c], Philippe Combette[c]

[a] Laboratoire TFT, École de technologie supérieure, Montréal, Québec H3C 1K3, Canada
[b] LMFA, UMR CNRS 5509, École Centrale de Lyon, 69134 Ecully Cedex, France
[c] IES, UMR CNRS 5214, Université de Montpellier, 34095 Montpellier Cedex 5, France

ARTICLE INFO

Article history:
Received 30 May 2017
Received in revised form 25 August 2017
Accepted 26 August 2017
Available online 1 September 2017

Keywords:
Shear-stress sensor
Thermal sensor
Calorimetric sensor
Aerodynamic sensor

ABSTRACT

The static calibration of two MEMS calorimetric shear-stress sensors is performed. In a first step, a calibration range of $\tau_w = \pm 2$ Pa is obtained in a two-dimensional channel-flow facility. The long-term repeatability of the sensors output, over a two-weeks period, is shown to be very good, with a standard deviation of less than 1% of the mean. In a second step, the sensors are calibrated in a large subsonic wind tunnel up to a velocity of 100 m/s, which corresponds to a range of $\tau_w = \pm 14$ Pa of wall shear-stress that is closer to realistic values in low-speed aerodynamic flows. A method to measure the frequency response of the calorimetric sensors is also proposed. At an average wall shear-stress of $\bar{\tau_w} = 1$ Pa, the sensors exhibit a cut-off frequency of approximately 1 kHz. Finally, the strong influence of the inter-beam distance on the static and dynamic characteristics of calorimetric sensors is demonstrated.[1]

1. Introduction

The friction stress caused by the flow of air over a solid surface is a fundamental parameter in aerodynamics. Beside being related to the total friction drag and hence to the performance of aerial and terrestrial vehicles, the local value of the wall shear-stress is a signature of flow physics occurring near the surface (*e.g.* laminar/turbulent transition, flow separation). Over the years, many types of shear-stress measurement devices have therefore been investigated, for example direct force sensors [1], indirect pressure sensors [2], or optical sensing of the deflection of micro-pillars [3]. Notwithstanding these developments, in practice the wall shear-stress on aerodynamic surfaces is still mainly measured with thermal sensors like near-wall hot wires [4] or more commonly hot-film sensors [5]. The main advantage of the hot film is its ruggedness compared to the hot wire. However, both types of sensors are insensitive to the flow direction, which can be a drawback when the detection of flow separation is required.

Recently, the authors introduced a new MEMS calorimetric shear-stress sensor for aerodynamic applications [6]. Contrary to hot wires or hot films, calorimetric sensors have the advantage of measuring the direction of the wall shear stress as well as its amplitude. On the other hand, the main drawback of calorimetric sensors is that their output is non monotonic, which implies that their range is necessarily limited [6,7]. In [6] the sensor prototype was tested up to a wall shear-stress of $\tau_w = \pm 1.2$ Pa. This is insufficient for most aerodynamic applications where the wall shear-stress can be of the order of tens of Pascal or even much more when the flow speed is increased. Furthermore, in addition to mean-flow measurements, shear-stress sensors can be used to measure the fluctuations of the wall shear-stress on the surface. This is particularly important when the flow state transitions from laminar to turbulent, or when the flow is fully turbulent [8]. Because turbulent fluctuations have a wide range of scales, this implies that the frequency response of the sensors must be characterized [9].

In this article we address these issues by first demonstrating the usefulness of the new MEMS calorimetric sensor in a larger range of wall shear-stress compared to [6] and second, by proposing a method to measure its frequency response when subjected to a fully turbulent flow.

2. Sensor design

Fig. 1 shows a sketch of our MEMS shear-stress sensor. Three horizontal beams are suspended over a small cavity. The middle beam, called the *heater*, is heated by an electrical current and the two side beams, called *detectors*, are used as resistance

* Corresponding author.
E-mail address: julien.weiss@etsmtl.ca (J. Weiss).

[1] An early version of this article was first presented at the 52nd 3AF International Conference on Applied Aerodynamics (Lyon, France) on March 29, 2017.

http://dx.doi.org/10.1016/j.sna.2017.08.048
0924-4247/

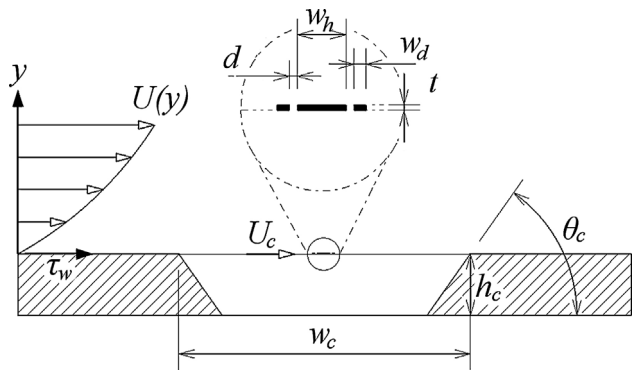

Fig. 1. Sketch of the MEMS calorimetric sensor (side view) [6].

thermometers. The flow of air over the heater generates a hot wake towards the downstream detector, whose resistance tends to increase compared to the upstream detector. The difference in electrical resistance between the two detectors is thus a measure of the wall shear-stress τ_w just upstream of the cavity. The sensor can be categorized as a *calorimetric* sensor since it essentially detects the asymmetry of the temperature profile around a heated element [7]. As explained in [6] the main advantage of calorimetric sensors compared to anemometric sensors like hot wires or hot films is that the former are direction sensitive, which means that they can detect the sign of the wall shear-stress as well as its magnitude.

Two new sensor prototypes were manufactured at IES-Montpellier using classical micro-fabrication techniques [6,10]. In both prototypes, the height of the cavity is $h_c = 400\,\mu m$, its width is $w_c = 1700\mu m$, and its length is $l_c = 2000\,\mu m$. The 0.8 μm thick beams are all made of a 500 nm layer of SiNx and a 300 nm layer of Pt. In between, a Cr_2O_3 or Ta_2O_5 adhesion-promoting layer is used [11]. In both prototypes, the width of the heater is $w_h = 50\,\mu m$. The differences between the two prototypes consist in the width w_d of the detectors and in the inter-beam distance d between heater and detectors. For prototype 1, $w_d = 10\,\mu m$ and $d = 10\,\mu m$, whereas for prototype 2, $w_d = 5\,\mu m$ and $d = 5\,\mu m$. In addition, prototype 2 features three SiNx support bridges between the heater and the detectors, in order to increase its mechanical resistance to the flow and to improve the flatness of the 3-beams system. Indeed, early testing with a third prototype with $l_c = 2000\,\mu m$, $w_d = 5\,\mu m$ and no support bridge demonstrated poor results because of the flexibility of the detectors. Fig. 2 shows a Scanning Electron Microscope (SEM) image of prototype 2 and Fig. 3 shows a zoom on one of the SiNx support bridges, which have a width of 10 μm. SEM images of prototype 1 are available in [6].

Both MEMS sensors were packaged on a 16-connector metallic support and bonded with aluminum wires. The support was itself secured on a machined plastic plug that can be inserted in a wind tunnel flush to a test surface (Fig. 4). For functional investigations, a dedicated electronic circuit was designed. It consists in a custom-built, constant-temperature anemometer (CTA) circuit for the heater and in a Wheatstone bridge for the detectors. The CTA circuit maintains the heater at an overheat ratio of $a_h = (R_h - R_a)/R_a = 0.7$ ($\Delta T = T_h - T_a \simeq 185\,^\circ C$), while the detectors are fed with a constant current of 2 mA for prototype 1 ($w_d = 10\,\mu m$) and 1 mA for prototype 2 ($w_d = 5\,\mu m$). In these relations the subscript h refers to the heater temperature and the subscript a to the air temperature. Note that the cold resistance of the heater is around 30 Ω and that of the detectors is roughly 130 Ω ($w_d = 10\,\mu m$, prototype 1) and 280 Ω ($w_d = 10\,\mu m$, prototype 2), respectively. The electronic circuit features two outputs: the *calorimetric output* E_{det} is proportional to the difference in the electrical resistance of the two detectors while the *anemometric output* E_{cta} is the output voltage of the CTA circuit. The latter output is useful because the heater wire can also be used as a relatively wide surface hot wire [4].

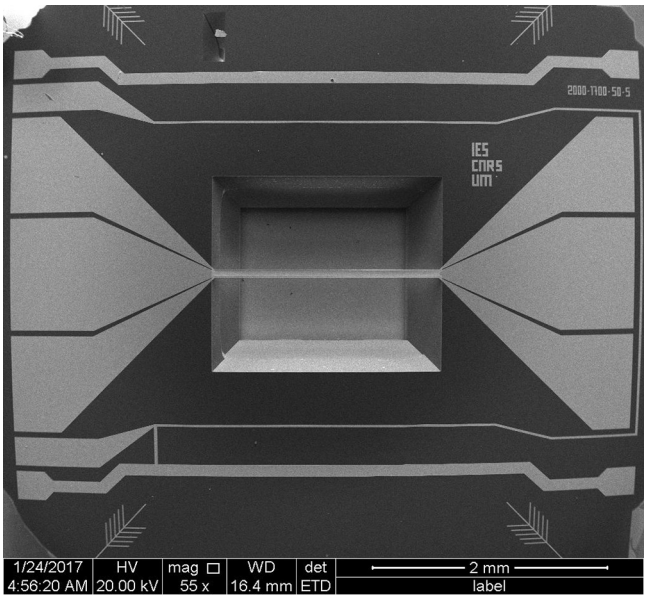

Fig. 2. SEM image of prototype 2.

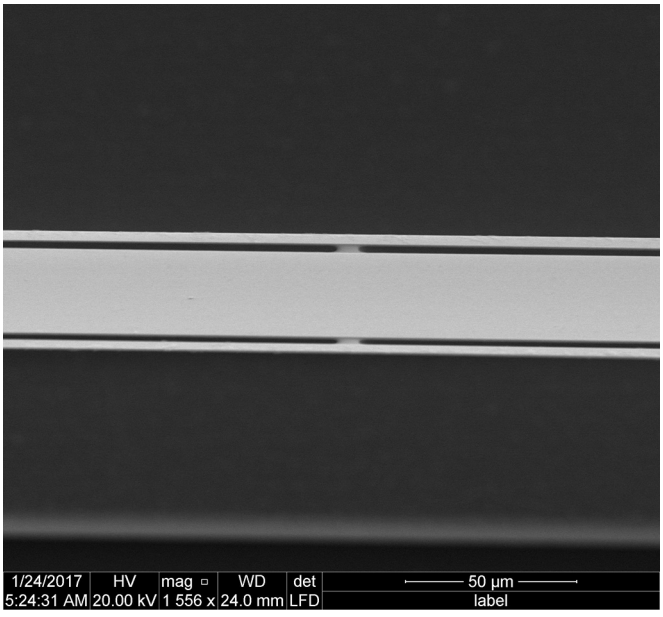

Fig. 3. SEM image of prototype 2, zoom on one support bridge.

3. Static calibration

The two sensor prototypes were first calibrated at ÉTS-Montréal in the two-dimensional channel flow facility pictured in Fig. 5. The channel has a length of 1.6 m, a height of 15 mm, and an aspect ratio of 11. The wall shear-stress in the channel is obtained from the measurement of the pressure gradient along its length, which gives a value within a few percent of what would be obtained with the more accurate technique of oil-film interferometry [12]. The maximum wall shear-stress achieved in the channel is $\tau_w = 2\,Pa$ and the flow is fully turbulent for $\tau_w > 0.1\,Pa$. For measurements of negative shear-stress, the sensor is rotated by 180°. Thus, the complete calibration range of the calorimetric sensor in the channel is $\tau_w = \pm 2\,Pa$. While this range of wall shear-stress is still relatively

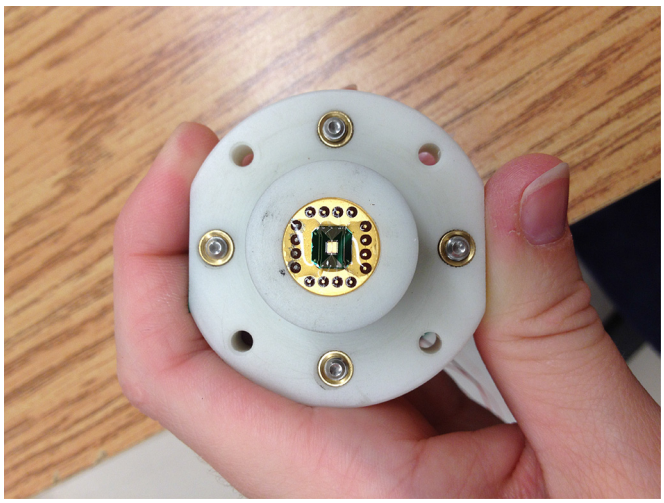

Fig. 4. MEMS sensor mounted in its plastic plug.

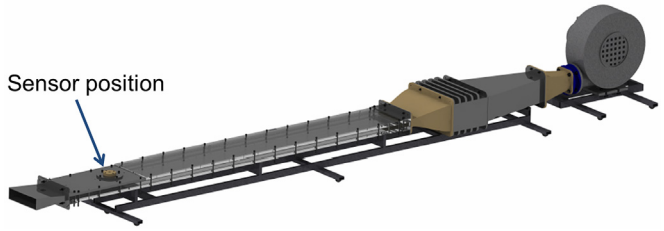

Fig. 5. ETS channel-flow facility.

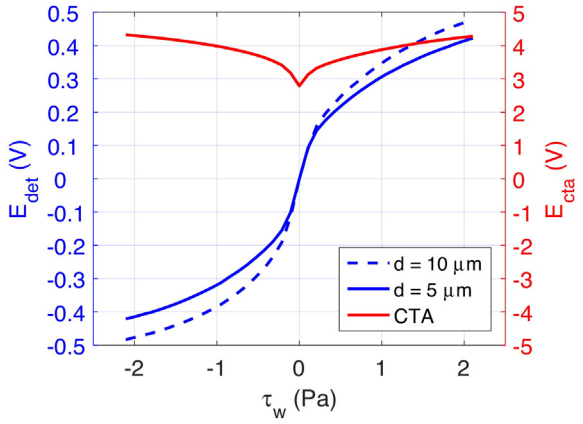

Fig. 6. Calibration curves in the range ±2 Pa. Blue curves: E_{det}, red curve: E_{cta}. (For interpretation of the references to color in this figure legend, the reader is referred to the web version of this article.)

limited for aerodynamic measurements, the channel-flow facility has the advantage of being inexpensive to use, which has enabled an investigation of the variability of the results, as will be discussed below.

Fig. 6 shows examples of the calibration curves obtained for the two sensor prototypes. The blue curves represent the calorimetric outputs E_{det}, which are a measure of the difference in electrical resistance of the two detectors. The red curve shows the anemometric output E_{cta}, which is almost identical for the two sensors since the dimensions of the central beams are the same. As already mentioned above, E_{cta} can be interpreted as the response of a surface hot wire since the heater is essentially a CTA-operated anemometric sensor. It can be seen in Fig. 6 that the E_{det} curves are approximately anti-symmetric, whereas the E_{cta} curve is symmetric with respect to the y axis. This illustrates the main advantage of calorimetric sensors compared to anemometric sensors, namely their sensitivity to the flow direction. The E_{det} and E_{cta} curves are both non linear, which is expected for anemometric as well as calorimetric sensors [7]. However, in the $\tau_w = \pm 2$ Pa range, the calorimetric output for both prototypes appears to be more sensitive than the anemometric output since the slope of both blue curves is everywhere larger than that of the red curve. Finally, the calorimetric sensor with $d = 10\,\mu$m (prototype 1) appears to be more sensitive than the sensor with $d = 5\,\mu$m (prototype 2). This is expected since it was showed in [6] that for relatively low values of τ_w, the sensitivity of calorimetric shear-stress sensors increases with the inter-beam distance d.

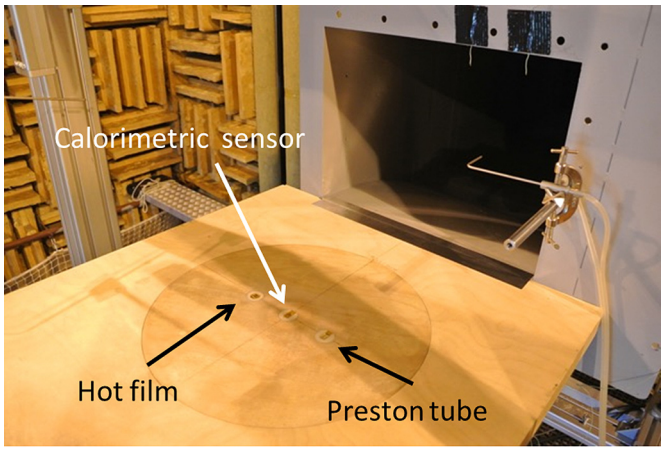

Fig. 7. Test section of the subsonic wind tunnel at ECL-LMFA.

Calibrations experiments similar to those shown in Fig. 6 were repeated for a total of twenty times over a two-weeks period with prototype 1. In some instances, the sensor was removed and reinstalled in the channel flow facility. The electronic circuit was also disconnected and reconnected between some tests. The standard deviation of the output voltage calculated over the 20 repeat runs was always less than 1% of its mean value in the $\tau_w = \pm 2$ Pa range, which demonstrates a very good repeatability of the sensor. Previous characterization experiments showed that the electrical resistance of the heater and detectors is stable within 0.01% [11].

The two sensor prototypes were also calibrated in the main subsonic wind tunnel of the Centre Acoustique at École Centrale de Lyon (ECL-LMFA) in France. In this facility, the flow is generated by a 850 kW Howden double-stage centrifugal blower delivering a nominal mass flow rate of 23 kg/s. Air passes through a settling chamber as well as through a honeycomb and several wire meshes designed to reduce free-stream turbulence. Acoustic treatment on the wind-tunnel walls and baffled silencers allow flow noise levels and contamination of the acoustic measurements performed in the anechoic chamber to be kept to a minimum. This results in an air flow at ambient temperature with a low background noise and low residual turbulence intensity, less than 0.5%. As shown in Fig. 7, the flow is finally guided into a large anechoic room of 10 m × 8 m × 8 m by a rectangular nozzle with a cross-section of 0.4 m by 0.3 m over a flat plate measuring 1.2 m in streamwise direction and 0.6 m in spanwise direction.

The MEMS calorimetric sensors were successively mounted on the centerline of the flat plate at a distance of 280 mm from the nozzle exit. The wall shear-stress on the plate was measured using a hot film and a Preston tube [13], each mounted at the same streamwise location but at ±60 mm on each side of the centerline (see Fig. 7). For some runs, an obstacle-wire sensor [14] was used in place of the Preston tube. Finally, the measured values of τ_w were verified through the use of Clauser's method on boundary-layer

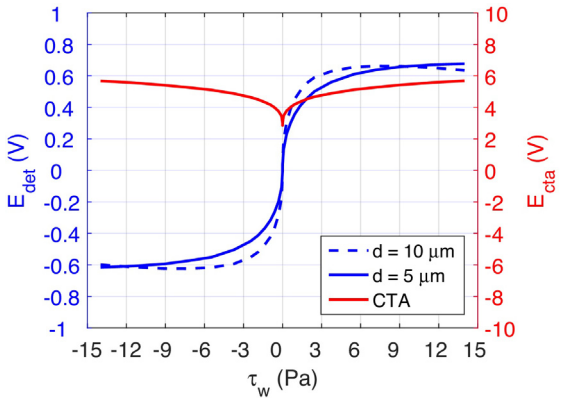

Fig. 8. Calibration curves in the range ±14 Pa. Blue curves: E_{det}, red curve: E_{cta}. (For interpretation of the references to color in this figure legend, the reader is referred to the web version of this article.)

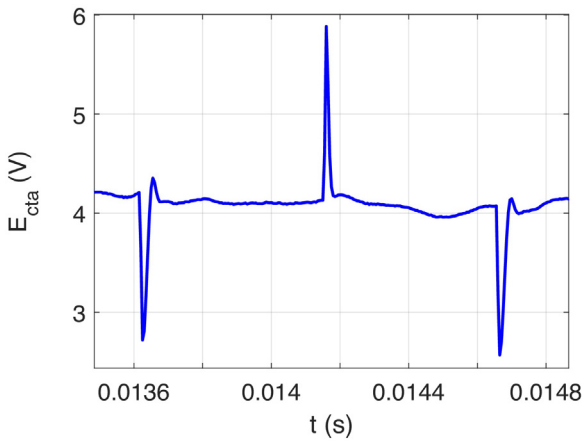

Fig. 9. CTA square-wave test, $\bar{\tau_w} = 1$ Pa.

velocity profiles measured with a hot-wire anemometer [13]. The maximum potential velocity of 100 m/s at the nozzle exit resulted in a maximum wall shear-stress of approximately 14 Pa at the sensor's position, thus increasing the calibration range by more than an order of magnitude compared to [6]. Based on a comparison between the different techniques that were used, the uncertainty in τ_w is estimated at ±5% in the wind tunnel. Note that here also, the sensor was rotated by 180° for measurements of negative shear-stress.

The calibration curves obtained in the subsonic wind tunnel are shown in Fig. 8. Generally speaking, the shape of the curves is consistent with those obtained in the calibration channel (Fig. 6). A noteworthy point is that the sensitivity of the calorimetric output clearly decreases with increasing wall shear-stress, as demonstrated by the decreasing character of the slope of both E_{det} curves. For prototype 1 ($d = 10$ µm), the calorimetric output even features a maximum at $\tau_w = 7$ Pa. Therefore, when the calorimetric output reaches this maximum, the wall shear-stress becomes undefined. This clearly shows that calorimetric sensors have a maximum range of wall shear-stress above which their output becomes ambiguous. As shown in [6] with simulations and experiments, this maximum range strongly depends on the inter-beam distance d: a smaller value of d implies a larger range. This is confirmed by the data of Fig. 8. For prototype 1 ($d = 10$ µm), the range is approximately 7 Pa but for prototype 2 ($d = 5$ µm), the range is larger than 14 Pa since the calorimetric output continues to increase at the edge of the domain. The inter-beam distance d thus appears to be a fundamental design parameter that affects both the range and sensitivity of calorimetric shear-stress sensors. Furthermore, the range of our prototype 2 ($d = 5$ µm) appears to be well suited for wall shear-stress measurements in aerodynamic flows up to 100 m/s. To the author's knowledge, such a large measurement range as never been achieved with a calorimetric shear-stress sensor before. This is essentially due to the smaller value of our inter-beam distance compared to typical sensors designed for mass-flow measurements [7].

4. Dynamic calibration

We now turn our attention to the dynamic behavior of the new MEMS sensors. When measurements of the fluctuating wall shear-stress under transitional or turbulent boundary layers are performed, the frequency response of sensors is fundamental for a correct interpretation of the results. For near-wall hot wires, the frequency response can generally be obtained using an electrical square-wave or sine-wave test, as with conventional hot wires [4]. For hot films, the interpretation of electrical tests is complicated by the thermal conduction towards the substrate and no reliable method currently exists [15,16]. In the case of calorimetric sensors, the authors are not aware of any existing theory either. The thermal problem is fairly complicated, since both conduction and convection of heat in the upstream and downstream directions need to be taken into account. Several one-dimensional models have been developed for calorimetric mass-flow sensors (*e.g.* [17–19]), but none is directly applicable to the current design.

In the present work we tackle the problem purely experimentally by using the output of the heater wire when the sensor is placed in a fully turbulent flow. As mentioned above, the heater is essentially a CTA-operated near-wall hot wire that produces a fluctuating output voltage under turbulent conditions. This means that the spectral characteristics of the fluctuating wall shear-stress – in the absence of any flow reversal – can be measured using the anemometric output. Furthermore, the cut-off frequency of the CTA can be obtained from a classical electrical square-wave test, and is typically of the order of a few tens of kHz [15]. Thus, by comparing the spectral characteristics of the calorimetric output with that of the anemometric output, the frequency response of the calorimetric output can be experimentally obtained.

Fig. 9 shows the square-wave response of the anemometric output E_{cta} at an average wall shear-stress of $\bar{\tau_w} = 1$ Pa. This was measured in the ÉTS two-dimensional channel flow facility (Fig. 5). The response was obtained by injecting a 1 kHz, 0.2 mA square-wave current signal into the diagonal of the Wheatstone bridge in the CTA circuit [20]. The width $\Delta t \simeq 30$ µs of the pulses indicates a cut-off frequency $f_c = 1/1.3\Delta t \simeq 25$ kHz according to Freymuth's criterion [15,20]. Thus, the spectral characteristics of the anemometric output are expected to be accurate up to this cut-off frequency. Note that the small asymmetry between the positive and negative pulses are most likely caused by non-linear effects and do not affect our conclusion [21].

Fig. 10 shows the power spectral density (PSD) of the fluctuating wall shear-stress τ'_w measured with both the anemometric and calorimetric outputs of prototype 1 ($d = 10$ µm), respectively. The data was again obtained at $\bar{\tau_w} = 1$ Pa but this time in the absence of any square-wave electrical input. The time traces of τ'_w were computed from the respective output voltages E_{cta} and E_{det} by fitting a fourth-order polynomial function to the calibration curves reported in Fig. 6, and by removing their respective mean value. The PSDs were computed using Welch's modified periodogram method using 256 averaging windows [22]. The time traces were measured for 180 s under fully turbulent flow conditions and the spectra were scaled to match the amplitudes at low frequency. It can be seen that the PSD of $(\tau'_w)_{det}$ faithfully follows that of $(\tau'_w)_{cta}$ up to approxi-

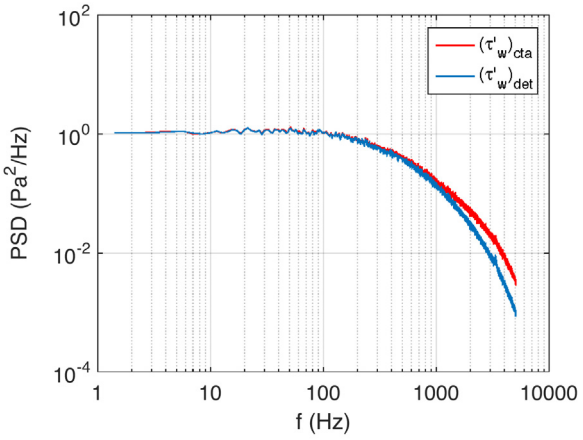

Fig. 10. PSD of fluctuating wall shear-stress measured with the anemometric output ($(\tau'_w)_{cta}$, red curve) and with the calorimetric output ($(\tau'_w)_{det}$, blue curve), $\bar{\tau_w} = 1$ Pa. (For interpretation of the references to color in this figure legend, the reader is referred to the web version of this article.)

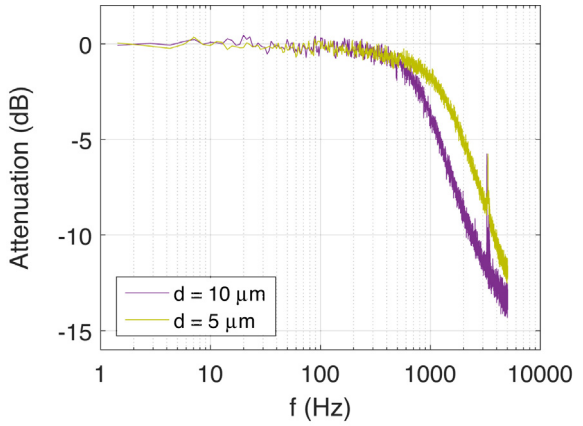

Fig. 11. Frequency response of the MEMS calorimetric sensors, $\bar{\tau_w} = 1$ Pa.

mately 1 kHz, above which the PSD of the calorimetric output is further attenuated. Since, as verified above, the cut-off frequency of the anemometric output is much higher than 1 kHz, we can conclude that the difference in the two PSDs is caused by the natural roll-off of the calorimetric output. Therefore, by dividing the two PSDs, the frequency response of the calorimetric output can be obtained.

The frequency response of both calorimetric MEMS sensors, measured using the above-described procedure and expressed in dB, is shown in Fig. 11. For both sensors the response is essentially flat until approximately 300 Hz, after which it starts to decrease. The decrease is more pronounced for the $d = 10$ μm sensor, with the −3 dB cut-off at 800 Hz. For the $d = 5$ μm sensor, the −3 dB cut-off is higher, at 1300 Hz. We conclude that the frequency response of the calorimetric sensor is lower than that of a CTA-operated near-wall hot wire. Nevertheless, at this value of the average wall shear-stress ($\bar{\tau_w} = 1$ Pa), the cut-off frequency improves when the inter-beam distance d decreases.

Sheplak et al. [23] suggested a required frequency response of 10 kHz for shear-stress sensors used in turbulence research. This is about an order of magnitude higher than what can be achieved with the current prototypes and it remains to be seen if such a frequency response could be attained by further reducing the inter-beam distance and optimizing the sensor dimensions. Furthermore, it should be mentioned that the current sensor dimensions are not adapted for the measurement of small-scale, near-wall turbulent fluctuations. At the maximum wall shear-stress attained in the wind tunnel ($\tau_w = 14$ Pa), the viscous length scale is $l_\nu \simeq 4$ μm, which is much smaller than the length of the beams and the height of the cavity. Nevertheless, the current prototypes, with their frequency response of approximately 1 kHz, are still quite useful for aerodynamic applications which do not necessarily require the accurate measurements of high-frequency turbulent fluctuations. These prototypes were for example used in [24] to investigate the low-frequency contraction and expansion of a turbulent separated flow.

5. Conclusion

The static and dynamic calibration of two MEMS calorimetric wall shear-stress sensors was performed. The sensors are made of three parallel beams mounted over a cavity, perpendicular to the flow direction. The central beam is maintained at a constant temperature while the electrical resistance of the two side detectors is measured and compared. The output voltage of the CTA circuit is referred to as the anemometric output while the difference in electrical resistance of the detectors is referred to as the calorimetric output.

The static calibration was first performed in a two-dimensional channel-flow facility for a range of $\tau_w = \pm 2$ Pa and second on a flat plate in a subsonic wind tunnel for a range of $\tau_w = \pm 14$ Pa. The inter-beam distance d between the heater and the detectors was shown to have a strong influence on the sensor's sensitivity and its measurement range, as already shown in a previous publication [6]. With an inter-beam distance of $d = 10$ μm, a measurement range of 7 Pa was achieved, whereas with an inter-beam distance of $d = 5$ μm, the measurement range exceeded 14 Pa. The repeatability of the sensor output over a 2-weeks period was shown to be very good, with a standard deviation of less than 1% of the mean.

A method to measure the frequency response of the calorimetric sensors was also proposed. It consists in measuring the cut-off frequency of the CTA-operated heater wire and comparing the spectral characteristics of both the anemometric and calorimetric outputs. For an average wall shear-stress of $\bar{\tau_w} = 1$ Pa, the $d = 10$ μm sensor was shown to have a cut-off frequency of approximately 800 Hz while the $d = 5$ μm sensor has a higher cut-off frequency of 1300 Hz. Further work is still required in order to investigate the variation of the frequency response with the average wall shear-stress.

Acknowledgments

The authors acknowledge the support of Mr. Jean Lyonnet (Université de Montpellier), who fabricated the MEMS sensor prototypes. They are also indebted to Mr. Michel Drouin (ÉTS Montréal) for his help in the design and manufacturing of the electronic circuit.

References

[1] V. Chandrasekharan, J. Sells, J. Meloy, D.P. Arnold, M. Sheplak, A microscale differential capacitive direct wall-shear-stress sensor, J. Microelectromech. Syst. 20 (3) (2011) 622–635.
[2] T. von Papen, U. Buder, H.D. Ngo, E. Obermeier, A second generation MEMS surface fence sensor for high resolution wall shear stress measurement, Sens. Actuators A: Phys. 113 (2) (2004) 151–155.
[3] S. Große, W. Schröder, Mean wall-shear stress measurements using the micro-pillar shear-stress sensor MPS3, Meas. Sci. Technol. 19 (1) (2008) 015403.
[4] D. Sturzebecher, S. Anders, W. Nitsche, The surface hot wire as a means of measuring mean and fluctuating wall shear stress, Exp. Fluids 31 (3) (2001) 294–301.
[5] T.R. Moes, G.R. Sarma, S.M. Mangalam, Flight demonstration of a shock location sensor using constant voltage hot-film anemometry, Tech. rep., NASA Technical Memorandum TM-4806, 1997.

[6] J. Weiss, Q. Schwaab, Y. Boucetta, A. Giani, C. Guigue, P. Combette, B. Charlot, Simulation and testing of a MEMS calorimetric shear-stress sensor, Sens. Actuators A: Phys. 253 (1) (2017) 210–217.
[7] M. Elwenspoek, R. Wiegerink, Mechanical Microsensors, Springer, 2001.
[8] C. Bailly, G. Comte-Bellot, Turbulence, Springer, 2015.
[9] V. Chandrasekaran, A. Cain, T. Nishida, L.N. Cattafesta, M. Sheplak, Dynamic calibration technique for thermal shear-stress sensors with mean flow, Exp. Fluids 39 (1) (2005) 56–65.
[10] F. Mailly, A. Giani, A. Martinez, R. Bonnot, P. Temple-Boyer, A. Boyer, Micromachined thermal accelerometer, Sens. Actuators A: Phys. 103 (3) (2003) 359–363.
[11] A. Garraud, P. Combette, A. Giani, Thermal stability of Pt/Cr and Pt/Cr_2O_3 thin-film layers on a SiNx/Si substrate for thermal sensor applications, Thin Solid Films 540 (2013) 256–260.
[12] R. Vinuesa, E. Bartrons, D. Chiu, K.M. Dressler, J.-D. Rüedi, Y. Suzuki, H.M. Nagib, New insight into flow development and two dimensionality of turbulent channel flows, Exp. Fluids 55 (6) (2014) 1759.
[13] S. Tavoularis, Measurements in Fluid Mechanics, 2005, Cambridge.
[14] N. Weiser, W. Nitsche, F. Renken, Wall shear stress determination by means of obstacle wires, Proc. of 8th Symposium of Turb. Shear Flows (1991) 4–5.
[15] H.H. Bruun, Hot-wire Anemometry: Principles and Signal Analysis, Oxford University Press, 1995.
[16] M. Sheplak, L. Cattafesta, T. Nishida, C.B. McGinley, MEMS Shear Stress Sensors: Promise and Progress, AIAA Paper 2004-2606, 2004.
[17] K. Komiya, F. Higuchi, K. Ohtani, Characteristics of a thermal gas flowmeter, Rev. Sci. Instrum. 59 (3) (1988) 477–479.
[18] N.T. Nguyen, W. Dötzel, Asymmetrical locations of heaters and sensors relative to each other using heater arrays: a novel method for designing multi-range electrocaloric mass-flow sensors, Sens. Actuators A: Phys. 62 (1–3) (1997) 506–512.
[19] W. Xu, K. Song, S. Ma, B. Gao, Y. Chiu, Y.-K. Lee, Theoretical and experimental investigations of thermoresistive micro calorimetric flow sensors fabricated by CMOS MEMS technology, J. Microelectromech. Syst. 25 (5) (2016) 954–962.
[20] P. Freymuth, Frequency response and electronic testing for constant-temperature hot-wire anemometers, J. Phys. E: Sci. Instrum. 10 (1977) 705–710.
[21] J. Weiss, A. Berson, G. Comte-Bellot, Investigation of nonlinear effects in constant-temperature anemometers, Meas. Sci. Technol. 24 (8) (2013) 085302.
[22] J.S. Bendat, A.G. Piersol, Random Data: Analysis and Measurement Procedures, 3rd ed., John Wiley & Sons, 2010.
[23] M. Sheplak, V. Chandrasekaran, A. Cain, T. Nishida, L.N. Cattafesta, Characterization of a silicon-micromachined thermal shear-stress sensor, AIAA J. 40 (6) (2002) 1099–1104.
[24] A. Le Floc'h, A. Mohammed-Taifour, J. Weiss, Investigation of the Low-Frequency Breathing Motion in Two Turbulent Separation Bubbles, AIAA Paper 2017-3970, 2017.

Biographies

Julien Weiss received an engineering degree from ENSMA Poitiers in 1997 and a Ph.D. in aerospace engineering from the University of Stuttgart in 2002. His main areas of scientific contributions are fluid mechanics and aerodynamic measurement technology. He also has a significant experience in aerodynamic wind-tunnel testing. He is currently Associate Professor at the Department of Mechanical Engineering at École de technologie supérieure in Montréal.

Emmanuel Jondeau received his university degree in technology from the UJF, Grenoble, in 1986 and the M.Sc. degree by being granted an equivalence from the French Interministerial Commission in 2004. Since 1992, he has been working in the Laboratoire de Mécanique des Fluides et d'Acoustique from the Ecole Centrale Lyon. He is currently a CNRS Engineer at the Center for Acoustics of the Laboratory. He is responsible for the design and setting up of complex experimental devices with main applications in the field of Fluid Mechanics and Acoustics. He has also a large experience in scientific instrumentation applied to aerodynamic measurements.

Alain Giani received his Ph.D. in electronics, optronics and systems from the University of Montpellier, France, in 1992. Since then, he has been working in the Institute of Electronics and Systems in the Montpellier University, as a specialist of microsensors and vacuum deposition techniques on materials for multiphysics detection and implementation in devices. Presently, he is involved in thermal microsensors for inertial measurements and pyro thin and thick films deposition.

Benoît Charlot was born in Vichy, France, in 1972. He received M.S and PhD degrees in microelectronics from the Institut National Polytechnique de Grenoble (INPG), France in 1996 and 2001, respectively. He is currently a researcher in CNRS (the French National Centre of the Scientific Research) and university of Montpellier within the IES laboratory (Institute of Electronics and Systems) in Montpellier, France. He is involved in MEMS, microfluidics, bioMEMS and biophysics.

Philippe Combette received his Ph.D. in electronics optronics and systems from the University of Montpellier, France, in 2000. Since then, he works in the Institut d'Electronique et des systémes from the University of Montpellier, where he is a specialist on sensors. Presently, he is involved in thermal microsensors and piezoelectric sensors for many applications.